CHINESE OPTICS LETTERS

Vol. 21, No. 9 | September 2023

High-gradient modulation of microbunchings using a minimized system driven by a vortex laser

Shufa Hao (郝书法)[1,2,3,†], Zhengxing Lv (吕政星)[1,3,†], Hao Dong (董 浩)[1,2,3], Jianzhi He (何坚志)[1,2,3], Nanshun Huang (黄楠顺)[3,4], Fengyu Sun (孙丰钰)[1,2,3], Zhiyong Shi (史志勇)[1], Hao Sun (孙 昊)[3,4], Wenpeng Wang (王文鹏)[1,3*], Yuxin Leng (冷雨欣)[1,3], Ruxin Li (李儒新)[1,2,3], and Zhizhan Xu (徐至展)[1**]

[1] State Key Laboratory of High Field Laser Physics and CAS Center for Excellence in Ultra-intense Laser Science, Shanghai Institute of Optics and Fine Mechanics, Chinese Academy of Sciences, Shanghai 201800, China

[2] School of Physical Science and Technology, ShanghaiTech University, Shanghai 201210, China

[3] University of Chinese Academy of Sciences, Beijing 100049, China

[4] Shanghai Institute of Applied Physics, Chinese Academy of Sciences, Shanghai 201800, China

*Corresponding author: wangwenpeng@siom.ac.cn

**Corresponding author: zzxu@mail.shcnc.ac.cn

Received April 17, 2023 | Accepted June 15, 2023 | Posted Online August 23, 2023

This study entailed the development of a high-gradient modulation of microbunching for traditional radiation frequency accelerators using a minimized system driven by a relativistic Laguerre–Gaussian (LG) laser in three-dimensional particle-in-cell (PIC) simulations. It was observed that the LG laser could compress the transverse dimension of the beam to within a 0.7 μm radius (divergence ≈ 4.3 mrad), which is considerably lower than the case tuned by a Gaussian laser. In addition, the electron beam could be efficiently modulated to a high degree of bunching effect (> 0.5) within ∼21 fs (∼7 μm) in the longitudinal direction. Such a high-gradient density modulation driven by an LG laser for pre-bunched, low-divergence, and stable electron beams provides a potential technology for the system minimization of X-ray free-electron lasers (XFELs) and ultrashort-scale (attosecond) electron diffraction research.

Keywords: relativistic Laguerre–Gaussian laser; electron bunch modulation; X-ray free-electron lasers.
DOI: 10.3788/COL202321.093801

1. Introduction

Owing to the requirement for high-quality electron beams or electromagnetic radiation in basic research fields[1], an increasing number of methods for improving their properties have been proposed and implemented. One of the major challenges in science is to observe atoms in motion with femtosecond time resolution[2,3] and angstrom spatial resolution[4,5]. Electron diffraction and synchrotron radiation have become indispensable detection methods for the study of ultrafast dynamics and ultra-high spatial resolution. However, they have weak coherence and pulses with long relaxation times, which is a big challenge for high-resolution spectroscopy and imaging experiments in the physical and chemical fields.

To solve these issues, advanced accelerator-based lights[6-9] and electronic compression mechanisms[10-12] have been developed to generate ultra-intense ultrafast full-coherence electron beams or radiation. For example, external nonrelativistic femtosecond Gaussian lasers[8,13,14] are usually combined with flexible magnetic devices[12,15,16] such as doglegs and magnetic chicanes to manipulate the relativistic electron distributions and precisely tailor the properties of the radiation pulse. First, a femtosecond Gaussian laser was used as an external seed to modulate the electron beam energy at the scale of the wavelength of the optical laser in the first undulator. Subsequently, a magnetic chicane (dispersion section) converts the formed energy modulation into an associated density modulation (microbunching)[17-21]. Finally, these electron microbunches are further input into the undulator to generate coherent harmonic emissions in the high-gain harmonic generation (HGHG)[22-24] or echo-enabled harmonic generation (EEHG)[25-29] schemes. During this process, beam control is an important factor for X-ray free-electron laser (XFEL) equipment, which usually depends on the complex insertion assembly and magnetic focusing devices. This equipment is considerably large and expensive; the development of a compact and economical mechanism for convenient XFEL applications is therefore needed.

One solution that has been implemented is to use the laser wake-field scheme driven by the relativistic Gaussian laser to accelerate electrons with extremely high acceleration gradient.

In the past decades, the relativistic vortex laser has drawn increasing attention in the laser acceleration. It has been theoretically verified that the Laguerre–Gaussian (LG) laser could generate collimated electron beams through the interaction with an ultrathin target[30,31]. Attosecond electron bunches generated from a nanofiber driven by LG lasers were also investigated[32–35].

2. Results and Discussion

In this study, strong coherent electron microbunching was realized by simply using an intense LG laser interacting with the beam source from a storage ring or traditional radio frequency gun in three-dimensional (3D) particle-in-cell (PIC) simulations. It can compact the energy and density modulation processes, from the large traditional magnetic chicanes and undulators, to tens of micrometers and femtoseconds. Studies have shown that electron beam density can be compressed from the initial density of $\sim 0.07 n_c$ to $\sim 0.7 n_c$ and the beam-bunching effect is sharply enhanced (>0.5) within the electron beam. In addition, the electron beam is accelerated from 1 MeV to hundreds of MeV with low divergence, which is expected to further compact the traditional accelerator section in future mimic XFEL facilities for various applications.

In 3D PIC simulations, a circularly polarized (CP) intense LG ($l=1, p=0, \sigma_z=-1$) laser was incident from the left boundary along the positive x-axis direction. The incident laser amplitude can be expressed as

$$\begin{aligned} \boldsymbol{E}_{\perp} = E_0 & \sqrt{\frac{2p!}{\pi(p+l)!}} \frac{1}{w(x)} \left[\frac{r\sqrt{2}}{w(x)}\right]^l \exp\left[\frac{r^2}{w^2(x)}\right] L_p^l\left[\frac{2r^2}{w^2(x)}\right] \\ & \times \exp(il\Phi) \exp\left[\frac{ik_0 r^2 x}{2(x^2+x_{\mathrm{R}}^2)}\right]\left[\boldsymbol{e}_y + \exp\left(\frac{i\pi\sigma_z}{2}\right)\boldsymbol{e}_z\right] \\ & \times \exp\left[-i(2p+l+1)\arctan\left(\frac{x}{x_{\mathrm{R}}}\right)+\varphi\right], \end{aligned} \tag{1}$$

where $E_0 = a_0 m_e \omega c/e$ is the dimensionless amplitude of the laser electric field; $a_0 = 40$ is the normalized laser intensity, which corresponds to a laser intensity of $\sim 7\times 10^{21}\ \mathrm{W/cm^2}$; e is the electron charge; m_e is the electron mass; ω is the laser frequency; and c is the speed of light in vacuum. $w(x) = w_0(1+x^2/x_{\mathrm{R}}^2)^{1/2}$ is the beam waist width of the laser; $w_0 = 4\ \mu\mathrm{m}$ is the full width at half-maximum of the laser focal spot; $x_{\mathrm{R}} = \pi w_0^2/\lambda$ is the Rayleigh length of the laser pulse; and $\sigma_z = -1$ represents the right CP mode. The laser pulse had a central wavelength $\lambda_0 = 0.8\ \mu\mathrm{m}$. The pulse width was approximately 30 fs. The duration of the incident electron beam duration was $7T$ ($T = \lambda_0/c$). The density of the electron beam was $n_e = 0.07 n_c$, and it was uniformly distributed in the range $-1\ \mu\mathrm{m} < y < 1\ \mu\mathrm{m}$ and $-1\ \mu\mathrm{m} < z < 1\ \mu\mathrm{m}$. The electrons within the beam have an initial energy of 1 MeV ($0.94c$), and the electron temperature was 8×10^4 eV. For the conventional accelerator electron beam divergence angle of 10^{-6} mrad, the initial divergence angle we set is 0 mrad, which is an ideal state. An incident laser pulse was injected at $t = 16T$. The grid scale of the simulation space was $1200\times 600\times 600$, and the corresponding coordinate length was $30\ \mu\mathrm{m}\ (x)\times 30\ \mu\mathrm{m}\ (y)\times 30\ \mu\mathrm{m}\ (z)$. The simulation used a moving window at time $t = 20T$, which moved along the laser direction at the speed of the light.

To show the detailed process of beam bunching, the 3D PIC code EPOCH[36] was used to simulate the relativistic LG laser propagation and its interaction with the input electron beam in Figs. 1(a) and 2. Previously, relativistic LG light was proposed using plasma holograms[37] or a large reflected phase plate for various applications in the laboratory[30,38,39]. In this study, the reflected scheme was devised to generate an intense LG laser ($\sim 7\times 10^{21}\ \mathrm{W/cm^2}$) to investigate the compact beam modulation system (see Fig. 1). It was found that the incident electron beam was cut into slices by the periodic concentrating and emanating electric fields in the transverse direction [see Fig. 1(d)] and oscillating acceleration fields in the longitudinal direction

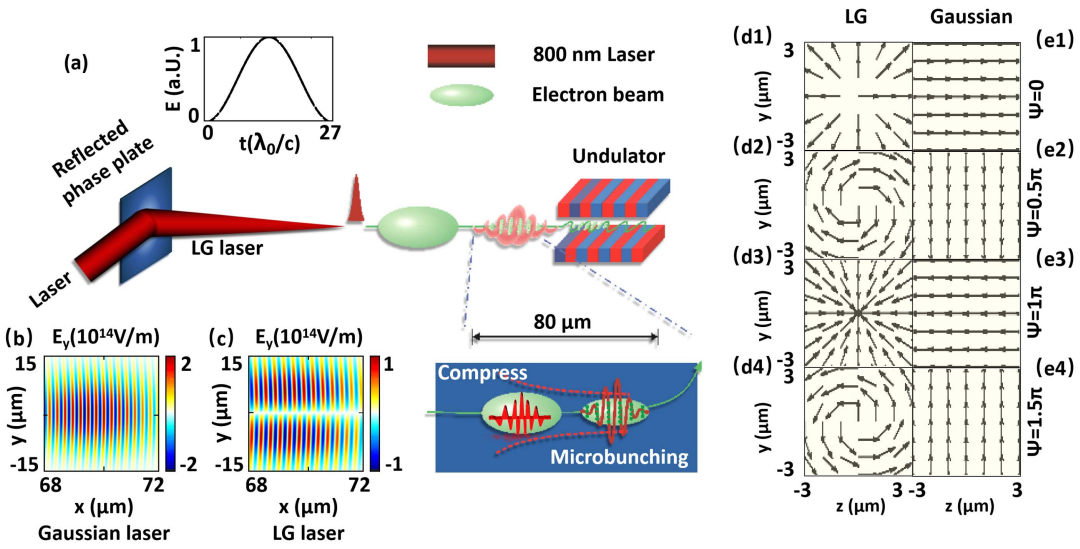

Fig. 1. (a) Schematic layout of the microbunching scheme and its potential application. (b), (c) Electric field (E_y) of LG and Gaussian laser. The corresponding vector plot of the electric fields for (d1)–(d4) LG_0^1 ($\sigma = -1$) and (e1)–(e4) Gaussian laser.

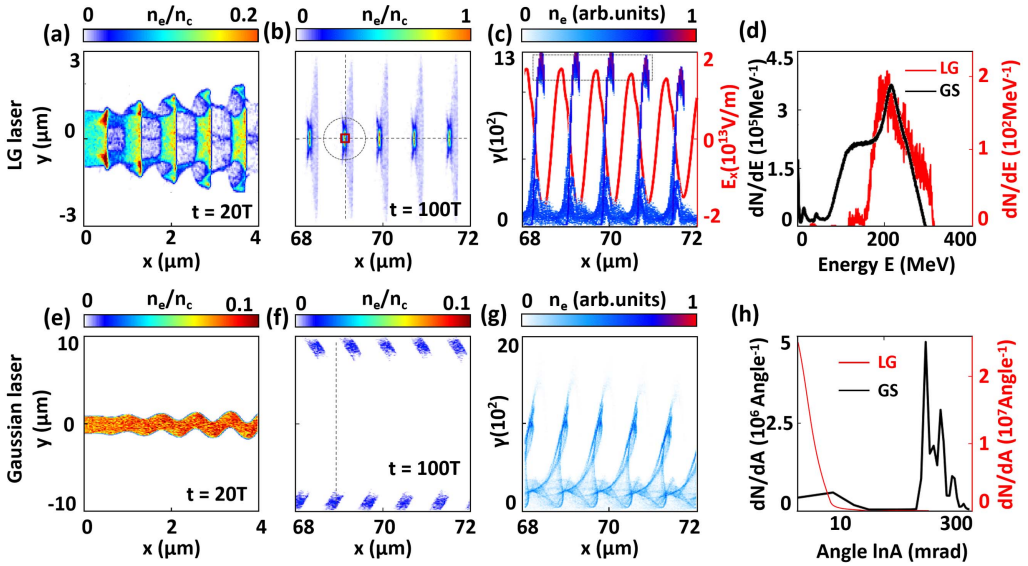

Fig. 2. (a), (b) Electron density maps generated by the LG laser at 20T and 100T. (e), (f) Electron density maps generated by the Gaussian laser under the same initial conditions as the LG laser. (c), (g) Longitudinal phase space distributions of electrons in (b) and (f). (d), (h) Comparison of the energy spectrum distribution and electron divergence generated by the LG and Gaussian lasers.

at $t = 20T$ [see Fig. 2(c)]. In contrast, the incident electron beam is sinusoidally distributed by a Gaussian sinusoidal electric field in the transverse direction [see Figs. 1(c) and 1(e)]. At $t = 100T$ (267 fs), a string of coherent microbunches was generated in the coherent duration of the laser wavelength λ_0 [see Fig. 2(b)] in the LG laser case, whereas the electron beam was transversely dispersed to a broadened region ($x = \pm 10\,\mu$m) for the Gaussian laser [see Fig. 2(f)]. The main reason for this is that the hollow intensity distribution of the LG laser provides a concentrating ponderomotive force for the electron beam in the central singularity, which finally bunches most of the electrons along the y axis ($-0.25\,\mu\text{m} < y < 0.25\,\mu$m) [see Fig. 2(b)]. Here, the divergence angle of each electron bunch is ~4.3 mrad, which is remarkably smaller than that in the case driven by the Gaussian laser [see Fig. 2(h)]. Notably, this beam collimation process is similar to the quadrupole magnet effect, which is used as an insertion device to focus the electron beam in conventional accelerators[40]. However, the quadrupole magnetic field length is on the submeter scale and is even larger in the superconducting quadrupole magnet[41]. The relativistic LG laser can generate an evident focusing effect at tens of micrometers, which can be considered to work as an "electron focusing lens," which may enable the miniaturization of conventional focusing systems in future experiments. Although this scheme can effectively compress the electron bunching, it cannot be directly applied in free-electron lasers (FELs) and requires further beam shaping.

In addition, the electron beam is modulated by the oscillating acceleration field E_x in the longitudinal direction, as shown in Fig. 2(c). This shows that $E_x \approx 10^{13}$ V/m can be obtained on the beam axis (x axis), which can reach the order of the accelerating field in the target normal sheath field acceleration mechanism[42], indicating that it can be used to efficiently accelerate electrons there. It is observed that most electrons are locked in the accelerating phase of E_x [Fig. 2(c)] and can be accelerated for hundreds of femtoseconds and hundreds of micrometers. At $t = 100T$, the central electron beam energy can reach up to 400 MeV, and its cutoff energy is slightly higher than the case driven by the Gaussian laser [see Fig. 2(b)]. However, the electron beam has been expanded to tens of micrometers in the transverse direction in the later Gaussian laser case, which requires further modulation and maintenance of the focusing state using quadrupole magnets. It is interesting that the hollow intensity distribution of the LG laser successfully resolves this issue, where the peak current intensity of the microbunching exceeds ten times the initial current at 100T [Fig. 3(a)]. Meanwhile, we could find that the charge and electron density distribution of adjacent microbunchings are similar [Fig. 3(a)], showing a Gaussian-like distribution in the transverse space. Therefore, the focusing effect of microbunchings located in the nearest phase is identical. The most important observation is that such dense electron slices can be continuously compressed, in the central oscillating electric field, to 0.12 μm (415 as), which is of great significance in the study of attosecond dynamics. The spot size of the laser also has an impact on the longitudinal morphology of the electron microbunching. An excessively large or small spot size can cause the broadening of the electron slice, which is related to the symmetry of the electric field along the optical axis. We select a relatively optimal solution with spot size of 4 μm here.

To understand the density modulation mechanism for the attosecond electron slice in the PIC simulations, we used a multi-particle model to calculate the one-dimensional electron motion on the beam axis (x axis). The initial longitudinal energies of the tested electrons were set to 1 MeV, which was similar to the simulation in Fig. 2. The one-dimensional longitudinal electric field along the x axis can be expressed as

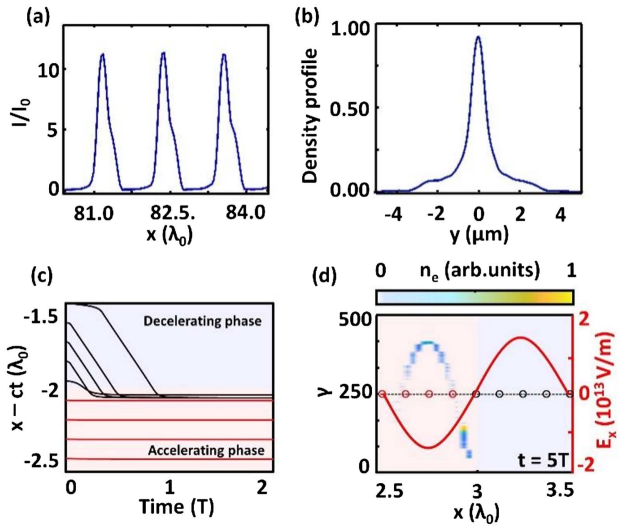

Fig. 3. (a) Current distribution modulated by the LG laser. Here, $\lambda_0 = 0.8$ μm. (b) Transverse electron distribution characteristics at 100T. (c) Trajectories of electrons in the multi-particle model. The black and red solid lines represent the electron trajectory in decelerating phase and accelerating phase, respectively. (d) Phase space distribution of electrons and longitudinal electric field (red line) distribution on the x axis at 5T (the hollow black circle represents the tested electrons with a uniform phase gap of 0.25π). Here, areas outlined in red and blue represent accelerating phase and decelerating phase, respectively.

$$E_x(x,t) = E_{\text{peak}}\cos(\omega t - kx + \pi/2), \quad -2.5\lambda_0 + ct < x < 2.5\lambda_0 + ct, \tag{2}$$

where $E_{\text{peak}} \approx 1.5 \times 10^{13}$ V/m is the peak amplitude of the laser electric field [see Fig. 3(c)]. Then, the particle acceleration and modulation can be expressed as follows:

$$\frac{\mathrm{d}}{\mathrm{d}t}\left(\frac{\beta}{\sqrt{1-\beta^2}}\right) = \frac{e}{m_e}E_x(x,t), \tag{3}$$

$$\frac{\mathrm{d}}{\mathrm{d}t}x(t) = \beta(t)c, \tag{4}$$

where E_x is the laser electric field, m_e is the electron mass, and $\beta = v/c$ is the dimensionless velocity. Nine typical electrons were uniformly distributed in the decelerating ($-2\lambda_0 < x < -1.5\lambda_0$) and accelerating phases ($-2.5\lambda_0 < x < -2\lambda_0$) in the E_x field [Fig. 3(c)]. It can be observed that electrons in the deceleration phase are dragged into the acceleration phase within 1T, and then stably accelerated by the positive electric field [Fig. 3(c)]. Meanwhile, the electrons initially in the acceleration phase are continuously accelerated and finally remain together with the electrons from the deceleration phase, resulting in a compressed electron layer, as shown in Fig. 3(d). All these results indicate that the electrons can be accelerated without dephasing for at least hundreds of femtoseconds, which can be proven by the dephasing rate R experienced by the accelerated electron in this study. For example, as indicated by Fig. 3(d), $R = (c - v_x)/c \sim 10^{-6}$ can be obtained at $t = 5T$, where v_x is the electron velocity, and the electric field E_x transports at light speed c, indicating that the electrons can be stably locked in the acceleration phase [Fig. 3(c)]. This is consistent with the simulation results shown in Fig. 2(c), which proves that the longitudinal electric field on the beam axis plays an important role in the acceleration and compression of the tuned electron beam.

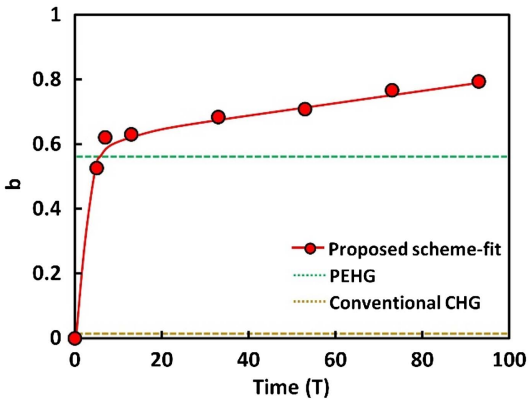

Fig. 4. Comparison of the degree of bunching effects produced using a conventional undulator (CHG)[22], PEHG scheme[13], and the method proposed in this study. The red solid line represents the fitting line of the bunching effect. The x axis represents the modulation time of the electron beam and laser field.

In synchrotron radiation applications, a higher bunching effect for electron beams is usually required to enhance the intensity of the output radiation using the coherent harmonic generation (CHG) technique[22,43]. A phase-merging enhanced harmonic generation (PEHG) mechanism has also been proposed to significantly increase the bunching factor [$\langle e^{i\theta}\rangle = \langle e^{i(k\bar{x}-\omega t+\varphi)}\rangle = \frac{1}{N}\sum_{i=1}^{N} e^{i(k\bar{x}-\omega t+\varphi)}$] by using a transverse-gradient undulator[13]. However, these methods require meter-scale devices. In our study, the LG laser could solve the miniaturization issue to a certain extent, where the electrons were directly tuned to a thin slice with a sharp bunching effect (~0.6) within 8T (~7 μm) (see Fig. 4). The electron-bunching effect can be further increased up to ~0.8 at $t = 100T$. Compared with the microbunching treatment in traditional undulators, the scheme driven by the LG laser has an evident microsize advantage. However, the energetic spectra in this study are slightly broader, which can be optimized by choosing an appropriate incident electron beam and LG laser parameters, as well as depending on the coordination of the complex achromatic system to further improve the quality of the electron beam.

3. Conclusions

In conclusion, a compact and low-cost scheme was proposed to generate ultrashort electron microbunching with a high bunching effect and low divergence using a relativistic LG laser without depending on large magnets and sophisticated connection

schemes of numerous insertion devices used in the traditional electronic modulation process. It was found that the incident electron beam density could be compressed to a near-critical density within a short time. The beam-bunching effect is sharply enhanced (>0.5), which is comparable to the compression mechanism in traditional accelerator systems. Simultaneously, the incident electron beam could be accelerated from 1 MeV to hundreds of MeV in tens of micrometers, which is expected to compact the traditional accelerator section. Due to the extreme sensitivity to energy dispersion in the application of FEL, the electron beam generated here is clearly unable to directly generate FEL radiation, which can be possibly improved by the mature beam compression schemes. In addition, the beam divergence could also remain at ~5 mrad in this study, similar to a quadrupole commonly used in synchrotron radiation. This may benefit the possible realization and applications of mimic XFEL facilities in the future.

Acknowledgement

This work was supported by the National Natural Science Foundation of China (No. 12075306), the Natural Science Foundation of Shanghai (No. 22ZR1470900), and Key Research Programs in Frontier Science (No. ZDBS-LY-SLH006).

†These authors contributed equally to this work.

References

1. Z. T. Zhao, "Storage ring light sources," Rev. Accel Sci. Technol. **3**, 57 (2010).
2. X. Wu, L. Z. Tan, X. Shen, T. Hu, K. Miyata, M. T. Trinh, R. Li, R. Coffee, S. Liu, D. A. Egger, I. Makasyuk, Q. Zheng, A. Fry, J. S. Robinson, M. D. Smith, B. Guzelturk, H. I. Karunadasa, X. Wang, X. Zhu, L. Kronik, A. M. Rappe, and A. M. Lindenberg, "Light-induced picosecond rotational disordering of the inorganic sublattice in hybrid perovskites," Sci. Adv. **3**, e1602388 (2017).
3. J. Li, W. G. Yin, L. Wu, P. Zhu, T. Konstantinova, J. Tao, J. Yang, S.-W. Cheong, F. Carbone, J. A. Misewich, J. P. Hill, X. Wang, R. J. Cava, and Y. Zhu, "Dichotomy in ultrafast atomic dynamics as direct evidence of polaron formation in manganites," npj Quantum Mater. **1**, 16026 (2016).
4. T. J. A. Wolf, D. M. Sanchez, J. Yang, R. M. Parrish, J. P. F. Nunes, M. Centurion, R. Coffee, J. P. Cryan, M. Gühr, K. Hegazy, A. Kirrander, R. K. Li, J. Ruddock, X. Shen, T. Vecchione, S. P. Weathersby, P. M. Weber, K. Wilkin, H. Yong, Q. Zheng, X. J. Wang, M. P. Minitti, and T. J. Martínez, "The photochemical ring-opening of 1,3-cyclohexadiene imaged by ultrafast electron diffraction," Nat. Chem. **11**, 504 (2019).
5. J. Yang, X. Zhu, T. J. A. Wolf, Z. Li, J. P. F. Nunes, R. Coffee, J. P. Cryan, M. Gühr, K. Hegazy, T. F. Heinz, K. Jobe, R. Li, X. Shen, T. Veccione, S. Weathersby, K. J. Wilkin, C. Yoneda, Q. Zheng, T. J. Martinez, M. Centurion, and X. Wang, "Imaging CF_3I conical intersection and photodissociation dynamics with ultrafast electron diffraction," Science **361**, 64 (2018).
6. P. Emma, R. Akre, J. Arthur, R. Bionta, C. Bostedt, J. Bozek, A. Brachmann, P. Bucksbaum, R. Coffee, F.-J. Decker, Y. Ding, D. Dowell, S. Edstrom, A. Fisher, J. Frisch, S. Gilevich, J. Hastings, G. Hays, Ph. Hering, Z. Huang, R. Iverson, H. Loos, M. Messerschmidt, A. Miahnahri, S. Moeller, H.-D. Nuhn, G. Pile, D. Ratner, J. Rzepiela, D. Schultz, T. Smith, P. Stefan, H. Tompkins, J. Turner, J. Welch, W. White, J. Wu, G. Yocky, and J. Galayda, "First lasing and operation of an angstrom-wavelength free-electron laser," Nat. Photonics **4**, 641 (2010).
7. R. W. Schoenlein, S. Chattopadhyay, H. H. W. Chong, T. E. Glover, P. A. Heimann, C. V. Shank, A. A. Zholents, and M. S. Zolotorev, "Generation of femtosecond pulses of synchrotron radiation," Science **287**, 2237 (2000).
8. X. Deng, A. Chao, J. Feikes, A. Hoehl, W. Huang, R. Klein, A. Kruschinski, J. Li, A. Matveenko, Y. Petenev, M. Ries, C. Tang, and L. Yan, "Experimental demonstration of the mechanism of steady-state microbunching," Nature **590**, 576 (2021).
9. X. Xu, F. Li, F. S. Tsung, K. Miller, V. Yakimenko, M. J. Hogan, C. Joshi, and W. B. Mori, "Generation of ultrahigh-brightness pre-bunched beams from a plasma cathode for X-ray free-electron lasers," Nat. Commun. **13**, 3364 (2022).
10. T. Van Oudheusden, P. L. E. M. Pasmans, S. B. Van Der Geer, M. J. de Loos, M. J. Van Der Wie, and O. J. Luiten, "Compression of subrelativistic space-charge-dominated electron bunches for single-shot femtosecond electron diffraction," Phys. Rev. Lett. **105**, 264801 (2010).
11. J. Maxson, D. Cesar, G. Calmasini, A. Ody, P. Musumeci, and D. Alesini, "Direct measurement of sub-10 fs relativistic electron beams with ultralow emittance," Phys. Rev. Lett. **118**, 154802 (2017).
12. K. L. F. Bane, F. J. Decker, Y. Ding, D. Dowell, P. Emma, J. Frisch, Z. Huang, R. Iverson, C. Limborg-Deprey, H. Loos, H. D. Nuhn, D. Ratner, G. Stupakov, J. Turner, J. Welch, and J. Wu, "Measurements and modeling of coherent synchrotron radiation and its impact on the linac coherent light source electron beam," Phys. Rev. Spec. Top. Accel. Beams **12**, 030704 (2009).
13. H. Deng and C. Feng, "Using off-resonance laser modulation for beam-energy-spread cooling in generation of short-wavelength radiation," Phys. Rev. Lett. **111**, 084801 (2013).
14. X. J. Deng, A. W. Chao, J. Feikes, W. H. Huang, M. Ries, and C. X. Tang, "Single-particle dynamics of microbunching," Phys. Rev. Accel. Beams **23**, 044002 (2020).
15. R. D'Arcy, S. Wesch, A. Aschikhin, S. Bohlen, C. Behrens, M. J. Garland, L. Goldberg, P. Gonzalez, A. Knetsch, V. Libov, A. M. de la Ossa, M. Meisel, T. J. Mehrling, P. Niknejadi, K. Poder, J. H. Röckemann, L. Schaper, B. Schmidt, S. Schröder, C. Palmer, J. P. Schwinkendorf, B. Sheeran, M. J. V. Streeter, G. Tauscher, V. Wacker, and J. Osterhoff, "Tunable plasma-based energy dechirper," Phys. Rev. Lett. **122**, 034801 (2019).
16. C. Feng and Z. Zhao, "A storage ring based free-electron laser for generating ultrashort coherent EUV and X-ray radiation," Sci. Rep. **7**, 4724 (2017).
17. E. Allaria, D. Castronovo, P. Cinquegrana, P. Craievich, M. Dal Forno, M. B. Danailov, G. D'Auria, A. Demidovich, G. De Ninno, S. Di Mitri, B. Diviacco, W. M. Fawley, M. Ferianis, E. Ferrari, L. Froehlich, G. Gaio, D. Gauthier, L. Giannessi, R. Ivanov, B. Mahieu, N. Mahne, I. Nikolov, F. Parmigiani, G. Penco, L. Raimondi, C. Scafuri, C. Serpico, P. Sigalotti, S. Spampinati, C. Spezzani, M. Svandrlik, C. Svetina, M. Trovo, M. Veronese, D. Zangrando, and M. Zangrando, "Two-stage seeded soft-X-ray free-electron laser," Nat. Photonics **7**, 913 (2013).
18. L. DiMauro, A. Doyuran, W. Graves, R. Heese, E. D. Johnson, S. Krinsky, H. Loos, J. B. Murphy, G. Rakowsky, J. Rose, T. Shaftan, B. Sheehy, J. Skaritka, X. J. Wang, and L. H. Yu, "First SASE and seeded FEL lasing of the NSLS DUV FEL at 266 and 400 nm," Nucl. Instrum. Methods Phys. Res. A **507**, 15 (2003).
19. D. Garzella, T. Hara, B. Carré, P. Salières, T. Shintake, H. Kitamura, and M. E. Couprie, "Using VUV high-order harmonics generated in gas as a seed for a single pass FEL," Nucl. Instrum. Methods Phys. Res. A **528**, 502 (2004).
20. G. Lambert, T. Hara, D. Garzella, T. Tanikawa, M. Labat, B. Carre, H. Kitamura, T. Shintake, M. Bougeard, S. Inoue, Y. Tanaka, P. Salieres, H. Merdji, O. Chubar, O. Gobert, K. Tahara, and M.-E. Couprie, "Injection of harmonics generated in gas in a free-electron laser providing intense and coherent extreme-ultraviolet light," Nat. Phys. **4**, 296 (2008).
21. T. Togashi, E. J. Takahashi, K. Midorikawa, M. Aoyama, K. Yamakawa, T. Sato, A. Iwasaki, S. Owada, T. Okino, K. Yamanouchi, F. Kannari, A. Yagishita, H. Nakano, M. E. Couprie, K. Fukami, T. Hatsui, T. Hara, T. Kameshima, H. Kitamura, N. Kumagai, S. Matsubara, M. Nagasono, H. Ohashi, T. Ohshima, Y. Otake, T. Shintake, K. Tamasaku, H. Tanaka, T. Tanaka, K. Togawa, H. Tomizawa, T. Watanabe, M. Yabashi, and T. Ishikawa, "Extreme ultraviolet free electron laser seeded with high-order harmonic of Ti:sapphire laser," Opt. Express **19**, 317 (2011).
22. L.-H. Yu, M. Babzien, I. Ben-Zvi, L. F. Dimauro, A. Doyuran, W. Graves, E. Johnson, S. Krinsky, R. Malone, I. Pogorelsky, J. Skaritka, G. Rakowsky, L. Solomon, X. J. Wang, M. Woodle, V. Yakimenko, S. G. Biedron,

J. N. Galayda, E. Gluskin, J. Jagger, V. Sajaev, and I. Vasserman, "High-gain harmonic-generation free-electron laser," Science **289**, 932 (2000).
23. E. Allaria, R. Appio, L. Badano, W. A. Barletta, S. Bassanese, S. G. Biedron, A. Borga, E. Busetto, D. Castronovo, P. Cinquegrana, S. Cleva, D. Cocco, M. Cornacchia, P. Craievich, I. Cudin, G. D'Auria, M. Dal Forno, M. B. Danailov, R. De Monte, G. De Ninno, P. Delgiusto, A. Demidovich, S. Di Mitri, B. Diviacco, A. Fabris, R. Fabris, W. Fawley, M. Ferianis, E. Ferrari, S. Ferry, L. Froehlich, P. Furlan, G. Gaio, F. Gelmetti, L. Giannessi, M. Giannini, R. Gobessi, R. Ivanov, E. Karantzoulis, M. Lonza, A. Lutman, B. Mahieu, M. Milloch, S. V. Milton, M. Musardo, I. Nikolov, S. Noe, F. Parmigiani, G. Penco, M. Petronio, L. Pivetta, M. Predonzani, F. Rossi, L. Rumiz, A. Salom, C. Scafuri, C. Serpico, P. Sigalotti, S. Spampinati, C. Spezzani, M. Svandrlik, C. Svetina, S. Tazzari, M. Trovo, R. Umer, A. Vascotto, M. Veronese, R. Visintini, M. Zaccaria, D. Zangrando, and M. Zangrando, "Highly coherent and stable pulses from the Fermi seeded free-electron laser in the extreme ultraviolet," Nat. Photonics **6**, 699 (2012).
24. E. Allaria, D. Castronovo, P. Cinquegrana, P. Craievich, M. Dal Forno, M. B. Danailov, G. D'Auria, A. Demidovich, G. De Ninno, S. Di Mitri, B. Diviacco, W. M. Fawley, M. Ferianis, E. Ferrari, L. Froehlich, G. Gaio, D. Gauthier, L. Giannessi, R. Ivanov, B. Mahieu, N. Mahne, I. Nikolov, F. Parmigiani, G. Penco, L. Raimondi, C. Scafuri, C. Serpico, P. Sigalotti, S. Spampinati, C. Spezzani, M. Svandrlik, C. Svetina, M. Trovo, M. Veronese, D. Zangrando, and M. Zangrando, "Two-stage seeded soft-X-ray free-electron laser," Nat. Photonics **7**, 913 (2013).
25. G. Stupakov, "Using the beam-echo effect for generation of short-wavelength radiation," Phys. Rev. Lett. **102**, 074801 (2009).
26. Z. T. Zhao, D. Wang, J. H. Chen, Z. H. Chen, H. X. Deng, J. G. Ding, C. Feng, Q. Gu, M. M. Huang, T. H. Lan, Y. B. Leng, D. G. Li, G. Q. Lin, B. Liu, E. Prat, X. T. Wang, Z. S. Wang, K. R. Ye, L. Y. Yu, H. O. Zhang, J. Q. Zhang, M. Zhang, M. Zhang, T. Zhang, S. P. Zhong, and Q. G. Zhou, "First lasing of an echo-enabled harmonic generation free-electron laser," Nat. Photonics **6**, 360 (2012).
27. D. Xiang, E. Colby, M. Dunning, S. Gilevich, C. Hast, K. Jobe, D. McCormick, J. Nelson, T. O. Raubenheimer, K. Soong, G. Stupakov, Z. Szalata, D. Walz, S. Weathersby, and M. Woodley, "Evidence of high harmonics from echo-enabled harmonic generation for seeding X-ray free electron lasers," Phys. Rev. Lett. **108**, 024802 (2012).
28. E. Hemsing, M. Dunning, B. Garcia, C. Hast, T. Raubenheimer, G. Stupakov, and D. Xiang, "Echo-enabled harmonics up to the 75th order from precisely tailored electron beams," Nat. Photonics **10**, 512 (2016).
29. P. R. Ribič, A. Abrami, L. Badano, M. Bossi, H.-H. Braun, N. Bruchon, F. Capotondi, D. Castronovo, M. Cautero, P. Cinquegrana, M. Coreno, M. E. Couprie, I. Cudin, M. B. Danailov, G. De Ninno, A. Demidovich, S. Di Mitri, B. Diviacco, W. M. Fawley, C. Feng, M. Ferianis, E. Ferrari, L. Foglia, F. Frassetto, G. Gaio, D. Garzella, A. Ghaith, F. Giacuzzo, L. Giannessi, V. Grattoni, S. Grulja, E. Hemsing, F. Iazzourene, G. Kurdi, M. Lonza, N. Mahne, M. Malvestuto, M. Manfredda, C. Masciovecchio, P. Miotti, N. S. Mirian, I. P. Nikolov, G. M. Penco, G. Penn, L. Poletto, M. Pop, E. Prat, E. Principi, L. Raimondi, S. Reiche, E. Roussel, R. Sauro, C. Scafuri, P. Sigalotti, S. Spampinati, C. Spezzani, L. Sturari, M. Svandrlik, T. Tanikawa, M. Trovó, M. Veronese, D. Vivoda, D. Xiang, M. Zaccaria, D. Zangrando, M. Zangrando, and E. M. Allaria, "Coherent soft X-ray pulses from an echo-enabled harmonic generation free-electron laser," Nat. Photonics **13**, 555 (2019).
30. W. P. Wang, C. Jiang, H. Dong, X. M. Lu, J. F. Li, R. J. Xu, Y. J. Sun, L. H. Yu, Z. Guo, X. Y. Liang, Y. X. Leng, R. X. Li, and Z. Z. Xu, "Hollow plasma acceleration driven by a relativistic reflected hollow laser," Phys. Rev. Lett. **125**, 034801 (2020).
31. Y. Shi, D. R. Blackman, and A. Arefiev, "Electron acceleration using twisted laser wavefronts," Plasma Phys. Control. Fusion **63**, 125032 (2021).
32. L. X. Hu, T. P. Yu, H. Z. Li, Y. Yin, P. McKenna, and F. Q. Shao, "Dense relativistic electron mirrors from a Laguerre–Gaussian laser-irradiated micro-droplet," Opt. Lett. **43**, 2615 (2018).
33. L. X. Hu, T. P. Yu, Z. M. Sheng, J. Vieira, D. B. Zou, Y. Yin, P. McKenna, and F. Q. Shao, "Attosecond electron bunches from a nanofiber driven by Laguerre–Gaussian laser pulses," Sci. Rep. **8**, 7282 (2018).
34. L.-X. Hu, T.-P. Yu, Y. Lu, G.-B. Zhang, D.-B. Zou, H. Zhang, Z.-Y. Ge, Y. Yin, and F.-Q. Shao, "Dynamics of the interaction of relativistic Laguerre–Gaussian laser pulses with a wire target," Plasma Phys. Control. Fusion **61**, 025009 (2019).
35. C. Baumann and A. Pukhov, "Electron dynamics in twisted light modes of relativistic intensity," Phys. Plasmas **25**, 083114 (2018).
36. T. D. Arber, K. Bennett, C. S. Brady, A. Lawrence-Douglas, M. G. Ramsay, N. J. Sircombe, P. Gillies, R. G. Evans, H. Schmitz, A. R. Bell, and C. P. Ridgers, "Contemporary particle-in-cell approach to laser-plasma modelling," Plasma Phys. Control. Fusion **57**, 113001 (2015).
37. A. Leblanc, A. Denoeud, L. Chopineau, G. Mennerat, P. Martin, and F. Quéré, "Plasma holograms for ultrahigh-intensity optics," Nat. Phys. **13**, 440 (2017).
38. Z. X. Zhang, C. Jiang, H. Dong, Z. Y. Shi, J. Z. He, S. F. Hao, F. Y. Sun, J. Y. Gui, J. Y. Qian, J. C. Zhu, W. P. Wang, Y. Xu, X. Y. Liang, Y. X. Leng, and R. X. Li, "Generation and application of high-contrast laser pulses using plasma mirror in the sulf-1pw beamline," Chin. Opt. Lett. **21**, 043802 (2022).
39. C. Jiang, W. P. Wang, S. Weber, H. Dong, Y. X. Leng, R. X. Li, and Z. Z. Xu, "Direct acceleration of an annular attosecond electron slice driven by near-infrared Laguerre–Gaussian laser," High Power Laser Sci. Eng. **9**, e44 (2021).
40. M. Johansson, B. Anderberg, and L.-J. Lindgren, "Magnet design for a low-emittance storage ring," J. Synchrotron Radiat. **21**, 884 (2014).
41. G. Le Bec, J. Chavanne, F. Villar, C. Benabderrahmane, S. Liuzzo, J. F. Bouteille, L. Goirand, L. Farvacque, J. C. Biasci, and P. Raimondi, "Magnets for the ESRF diffraction-limited light source project," IEEE Trans. Appl. Supercond. **26**, 4000107 (2016).
42. J. Fuchs, P. Antici, E. d'Humières, E. Lefebvre, M. Borghesi, E. Brambrink, C. A. Cecchetti, M. Kaluza, V. Malka, M. Manclossi, S. Meyroneinc, P. Mora, J. Schreiber, T. Toncian, H. Pépin, and P. Audebert, "Laser-driven proton scaling laws and new paths towards energy increase," Nat. Phys. **2**, 48 (2006).
43. B. Girard, Y. Lapierre, J. M. Ortega, C. Bazin, M. Billardon, P. Elleaume, M. Bergher, M. Velghe, and Y. Petroff, "Optical frequency multiplication by an optical klystron," Phys. Rev. Lett. **53**, 2405 (1984).